ELSEVIER

Journal of Contaminant Hydrology 17 (1995) 239–273

JOURNAL OF
Contaminant
Hydrology

The potential for metal release by reductive dissolution of weathered mine tailings

I. Ribet[a], C.J. Ptacek[b,c], D.W. Blowes[c], J.L. Jambor[c,α,*]

[a]*École des Mines de Paris, Centre d'Informatique Géologique, 35 rue St. Honoré, F-77305 Fontainebleau, France*

[b]*National Water Research Institute, 867 Lakeshore Road, P.O. Box 5050, Burlington, Ont. L7R 4A6, Canada*

[c]*Waterloo Centre for Groundwater Research, University of Waterloo, Waterloo, Ont. N2L 3G1, Canada*

Received 3 November 1992; revision accepted 15 February 1994

Abstract

Remediation programs proposed for decommissioned sulphide tailings may include the addition of a cover layer rich in organic-carbon material such as sewage sludge or composted municipal waste. These covers are designed to consume oxygen and prevent the oxidation of underlying sulphide minerals. The aerobic and anaerobic degradation of such organic-carbon-rich waste can release soluble organic compounds to infiltrating precipitation water. In laboratory experiments, and in natural settings, biotic and abiotic interactions between similar dissolved organic compounds and ferric-bearing secondary minerals have been observed to result in the reductive dissolution of ferric (oxy)hydroxides and the release of ferrous iron to pore waters. In weathered tailings, oxidation of sulphide minerals typically results in the formation of abundant ferric-bearing secondary precipitates near the tailings surface. These secondary precipitates may contain high concentrations of potentially toxic metals, either coprecipitated with or adsorbed onto ferric (oxy)hydroxides. Reductive dissolution reactions, resulting from the addition of the organic-carbon covers, may remobilize metals previously attenuated near the tailings surface. To assess the potential for metal release to tailings pore water by reductive dissolution reactions, a laboratory study was conducted on weathered tailings collected from the Nickel Rim mine tailings impoundment near Sudbury, Ontario, Canada. This site was selected for study because it is representative of many tailings sites. Mineralogical study indicates that sulphide minerals originally present in the vadose zone at the time of tailings deposition have been replaced by a series of secondary precipitates. The most abundant secondary minerals are goethite, gypsum and jarosite. Scanning electron microscopy, coupled with elemental analyses by X-ray energy dispersion analysis, and electron microprobe analysis indicate that trace metals including Ni, Cr and Cu are associated with these secondary minerals. To assess the masses of trace metals associated with each of the

[α] Formerly, Environmental Laboratory, CANMET, 555 Booth St., Ottawa, Ont. K1A 0G1, Canada

SSDI 0169-7722(94)00010-F

dominant secondary mineral phases, a series of extraction procedures was used. The masses of metals determined in three fractions (water soluble, reducible and residual) suggest that the greatest accumulation of metals is in the reducible fraction. These measurements indicate that high concentrations of metals are potentially available for release by reductive dissolution of the ferric-bearing secondary minerals. The actual mass of metals that can be released by this mechanism will depend on a number of site-specific characteristics, particularly the intensity of the reducing conditions established near the tailings surface.

1. Introduction

Since the discovery of sulphide ore in the Sudbury basin of Ontario, Canada, in 1883, the district has become one of the largest mining centres in the world, producing nickel, copper, cobalt, silver, gold, platinum-group metals, and other commodities. The Nickel Rim mine area, located in the Sudbury basin (Fig. 1) was selected for study because its tailings are representative of many others generated by the mining and milling of massive sulphide ores (Blowes, 1990; Blowes and Jambor, 1990; Blowes et al., 1991, 1992).

Since tailings deposition ended in early 1958, the water table in the Nickel Rim tailings impoundment has fallen, allowing the entry of gas-phase O_2, resulting in the

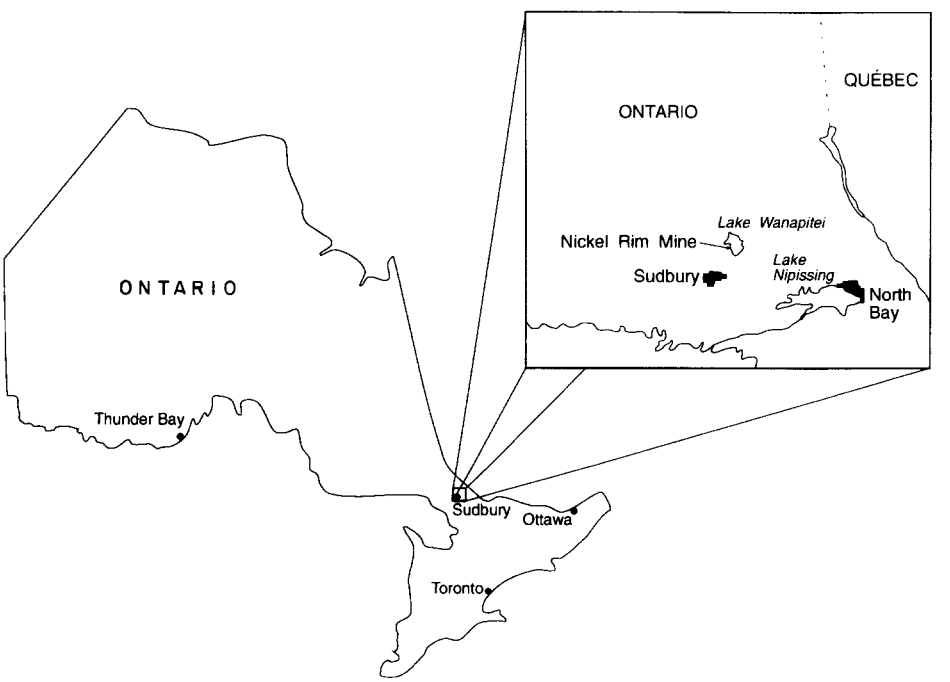

Fig. 1. Map showing the location of Nickel Rim mine tailings impoundment, near Sudbury, Ontario, Canada.

oxidation of sulphide minerals in the shallow tailings (Fig. 2). Sulphide oxidation is evident by the reddish-brown colour of the shallow tailings and by the discharge of acidic water from margins of the tailings impoundment. In addition to generating low-pH conditions, sulphide oxidation has led to the precipitation of large masses of ferric-bearing secondary minerals. These minerals contain high concentrations of potentially toxic metals.

Sulphide oxidation and acid mine drainage are observed at many tailings areas, and a variety of remediation programs is currently under study. One remediation approach proposed to mitigate acidic drainage is to cover the tailings with organic-carbon-rich materials such as sewage sludge, composted municipal waste, peat or sawdust (Blenkinsopp et al., 1991; Broman et al., 1991; Brown, 1991; Pitchel and Dick, 1991) (Fig. 3). These covers are designed to consume oxygen and prevent the oxidation of the underlying sulphide minerals. Because organic-carbon covers are relatively inexpensive and can be composed of a variety of wastes types, their use seems attractive. In some settings, however, aerobic and anaerobic degradation of organic-carbon-rich waste can release soluble organic compounds to infiltrating precipitation water. When this organic-rich water contacts tailings located below the organic cover, reductive dissolution of solid-phase ferric-bearing secondary precipitates, previously accumulated in the upper tailings materials, potentially can lead to the release of metals from the tailings site.

Facultative bacteria, commonly associated with organic-carbon-rich waters, are capable of oxidizing organic carbon at the expense of a series of electron donors including O_2, NO_3, Mn(IV), Fe(III) and SO_4. In general, these bacteria tend to catalyse the most energetically favourable reaction. As an oxidant is consumed, the

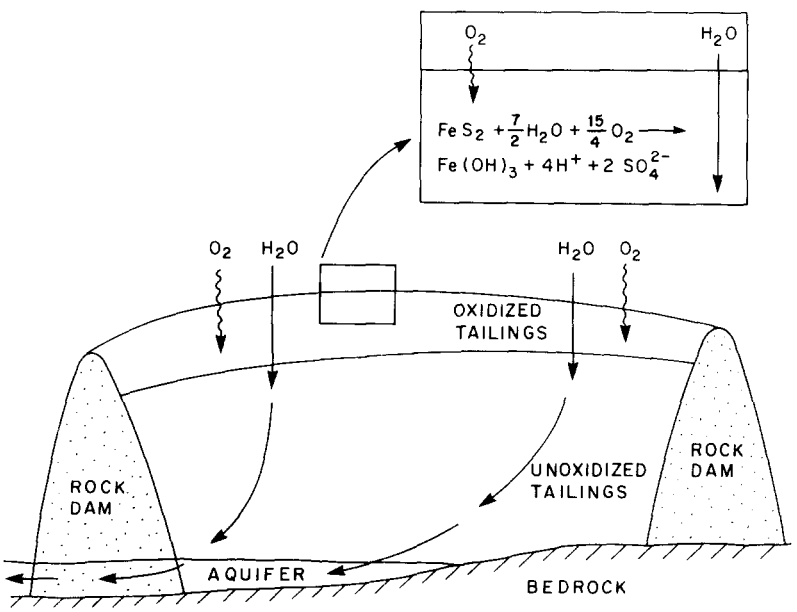

Fig. 2. Schematic diagram of an uncovered tailings impoundment.

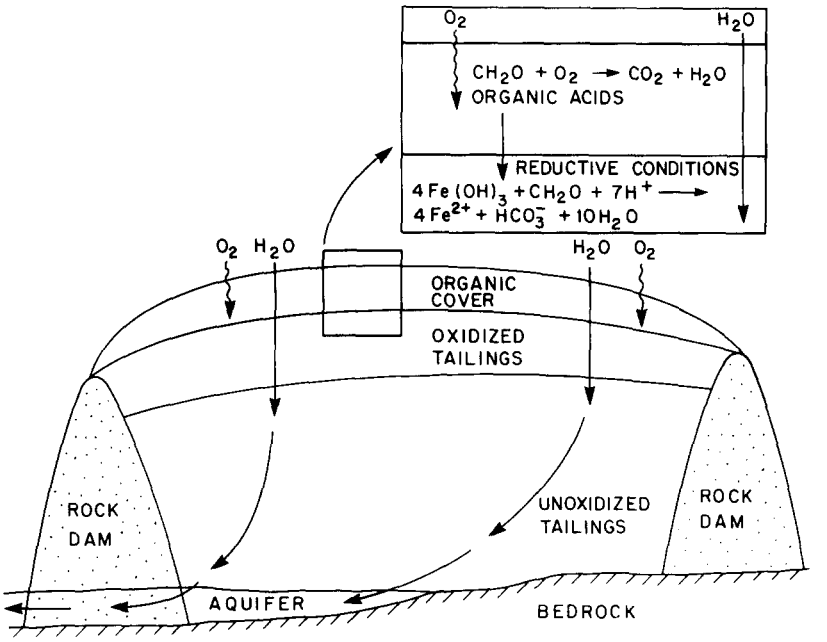

Fig. 3. Schematic diagram of a tailings impoundment covered with organic matter.

reduction of the subsequent oxidized species increases. The potential energy gain available to bacteria through an oxidation–reduction reaction is determined by the change in free energy for the reaction. The free energy changes for a series of reduction reactions associated with the oxidation of a simple organic compound, represented by CH_2O, are summarized in Table 1. The magnitudes of these free-energy changes suggest that at pH 7 these oxidants should be consumed in the order O_2, NO_3, Mn(IV), Fe(III), SO_4, and finally, organic carbon. Mine wastes below organic-carbon covers will be isolated from atmospheric O_2. In addition, NO_3 concentrations in inactive mine wastes are generally low (Blowes, 1990). The next two potential oxidants, Mn(IV) and Fe(III), are likely to be present within the mine wastes and, of these, Fe(III) in the form of Fe(III)-(oxy)hydroxides is abundant. Even at very low concentrations of dissolved organic carbon, the reduction of Fe(III) is thermodynamically favoured.

Studies on the reductive dissolution of oxide minerals by organic compounds, similar to those usually found in landfill leachates (Table 2), indicate that reductive dissolution of Mn-oxides, Co-oxides and Fe(III)-oxides occurs readily. These studies also indicate that, at low pH levels, Fe(III)-oxides participate in the same reactions with organic compounds as do Mn- or Co-oxides; Fe-oxides, however, are weaker oxidants (Stone and Ulrich, 1989). Fe(III)-oxides in natural environments can be reduced either directly or indirectly by bacteria (LaKind and Stone, 1989). Bacteria can participate directly in the reductive-dissolution reaction by using membrane-bound electron-transfer proteins to couple intercellular redox transfer processes to extracelluar iron reduction. Bacteria can also participate indirectly by accumulating

Table 1
Free energy for organic-matter oxidation using different electron acceptors

Process	Reaction[a]	Free energy[b] (kcal mol^{-1})
Denitrification	$CH_2O + 4/5NO_3^- \rightarrow 2/5N_{2(g)} + HCO_3^- + 1/5H^+ + 2/5H_2O$	−112.7
Mn(IV) reduction	$CH_2O + 2MnO_{2(s)} + 3H^+ \rightarrow 2Mn^{2+} + HCO_3^- + 2H_2O$	−84.9
Fe(III) reduction	$CH_2O + 4Fe(OH)_{3(s)} + 7H^+ \rightarrow 4Fe^{2+} + HCO_3^- + 10H_2O$	−26.8
Sulphate reduction	$CH_2O + 1/2SO_4^{2-} \rightarrow 1/2HS^- + HCO_3^- + 1/2H^+$	−23.9
Methane fermentation	$CH_2O + 1/2H_2O \rightarrow 1/2CH_4 + 1/2HCO_3^- + 1/2H^+$	−21.6

[a] Reactions from Freeze and Cherry (1979).
[b] Free energy data from Garrels and Christ (1965) and Brock et al. (1984); calculation for solution pH of 7.0.

biologically refractory compounds and excreting metabolites and other compounds that have reductive properties. Although thermodynamically favoured, the abiotic reductive dissolution of Fe(III)-oxides by landfill-derived short-chain organic acids is likely to be slow; biologically catalysed reduction using the same organic acids is expected to be much more rapid.

Microorganisms that reduce Fe(III) include *Pseudomonas* sp. *200* (Arnold et al., 1988), a member of the genus *Vibrio* (Jones et al., 1983, 1984), *Alteromonas putrefaciens* (Lovley et al., 1989b), and the microorganism GS-*15*, identified by Lovley and Phillips (1988), which completely oxidizes organic matter to carbon dioxide with the reduction of Fe(III) or Mn(IV). Several of these bacteria are common in a variety of natural systems. A number of organic compounds can serve as electron donors for these redox reactions, including acetate, propionate, butyrate, formate, lactate, ethanol (Lovley, 1987; Lovley and Phillips, 1988, 1989), and a variety of aromatic compounds, including toluene, phenol and *p*-cresol (Lovley

Table 2
Summary of studies on reductive dissolution of oxides by organic compounds

Oxides	Organic compounds	Authors
Goethite	oxalate	Zinder et al. (1986)
Hematite and goethite	oxalate	Suter et al. (1988)
Magnetite and hematite	ascorbate	Dos Santos Alfonso et al. (1990)
Goethite and hematite	phenolic reductants	LaKind and Stone (1989)
Mn(III)- and Mn(IV)-oxides	hydroquinone	Stone and Morgan (1984a)
Mn(III)- and Mn(IV)-oxides	27 aromatic and non-aromatic compounds	Stone and Morgan (1984b)
Mn(III)- and Mn(IV)-oxides	substituted phenols	Stone (1987a)
Mn(III)- and Mn(IV)-oxides	oxalate and pyruvate	Stone (1987b)
Mn(III)-dioxide and Co(III)-oxide	hydroquinone	Stone and Ulrich (1989)

et al., 1989a, b; Lovley and Lonergan, 1990). Many of these organic-carbon compounds were identified as common components of landfill leachates. Thus, it seems possible that these metal-oxide-reducing microorganisms could become established in tailings covered with similar organic waste materials, and that the Fe(III)-oxides contained in tailings may be biologically reduced in the same manner as in natural settings.

The objectives of the current study are: (1) to characterize and estimate the mass of ferric (oxy)hydroxide precipitates accumulated in the shallow vadose zone of the Nickel Rim mine tailings, the zone that potentially may be affected by reductive dissolution reactions; and (2) to estimate the masses of other metals that are associated with the ferric (oxy)hydroxides, that may be released to the pore water if the ferric (oxy)hydroxides are reductively dissolved.

Mineralogical study permits the identification of the primary and secondary mineral phases in the tailings and the distribution of the trace metals among the weathering products. The masses of trace metals associated with individual secondary mineral grains in the Nickel Rim mine tailings are variable. The determination of the masses of trace metals associated with the primary and secondary phases using mineralogical techniques requires extensive microscopic study of a representative number of mineral grains. Mineralogical techniques, therefore, are not well suited to characterize trace-metal contents of the secondary phases contained in bulk samples of the tailings solids.

Chemical extraction techniques have been used to help determine the masses of elements associated with classes of mineral phases present in soil materials and aquifer solids. These extraction techniques range from simple water-washing to remove soluble salts, to complex multiple-component chemical extraction schemes (Tessier et al., 1979) intended to separate trace metals on the basis of the chemical properties of the host mineral phases. Multiple-component extraction schemes have been the subject of much criticism (e.g., Tessier and Campbell, 1988, 1991; Nirel and Morel, 1990). The principal criticisms of extraction techniques are: the use of an extraction procedure a priori to classify components according to an operational category, the lack of adequate testing using standardized materials representative of field settings, and the assumption that metal masses liberated using harsh inorganic reagents are representative of those that can be released by biological mechanisms under natural conditions.

In the current study, a combined approach was taken to characterize the metal masses retained in the oxidized zone in the tailings. A detailed mineralogical examination of the tailings and the secondary weathering products was conducted to determine the dominant primary and secondary phases. Scanning electron microscope (SEM) study, coupled with elemental analysis by energy-dispersion X-ray analysis (EDXA), and electron-microprobe analysis were used to identify the locations of trace and heavy metals within the tailings. The results of the mineralogical study were then used to develop a sequential two-part extraction procedure. Using the results of the initial extractions, this procedure was simplified to a one-step procedure that separated the secondary sulphate and Fe(III)-(oxy)hydroxide portion of the tailings (reducible phase) from the primary sulphide and silicate portions

(residual phase). This extraction procedure was intended to separate the trace metals on the basis of their presence within the secondary oxide form vs. the primary sulphide and silicate minerals. This procedure was not intended to simulate a natural biological process in intensity or rate. The purpose, instead, was to separate the metals that are contained in phases potentially susceptible to bacterially-catalysed Fe(III)-(oxy)hydroxide mineral reduction (reducible phase) vs. those contained in the phases that are potentially susceptible to oxidation (residual phase).

2. Site description

Mining at the Nickel Rim mine, near Falconbridge, Ontario (Fig. 1), began in 1929, but a mill was not constructed at the mine site until 1953. Mine production was at ~690 t* day^{-1} until mine closure in early 1958. During mine operation, tailings were accumulated in a 9.4-ha elevated impoundment. The tailings range from <1 to 10.5 m in thickness, and have been subject to oxidizing conditions for about thirty years. The unoxidized tailings contain ~3 wt% S, primarily as pyrrhotite, ~0.1–0.2 wt% carbonates (reported as $CaCO_3$), with the remainder largely various silicates (Johnson, 1993).

3. Methods of investigation

3.1. Sample collection

Samples were collected from the Nickel Rim impoundment in 1991 and 1992, using the sampling technique of Starr and Ingleton (1992). The core samples were frozen shortly after collection and stored at −15°C until analysis. Core samples collected at four locations on the impoundment, NR*1*, NR*2*, NR*6* and NR*18* (Fig. 4), were used for the mineralogical study and the laboratory analysis. The samples were thawed and dried at room temperature and then divided into several subsamples, either according to physical observations of degree of oxidation (for NR*1* and NR*2*) or into 10-cm-long subsamples (for NR*6* and NR*18*). These subsamples were crushed by hand and homogenized before chemical extraction. Measurements of gas-phase O_2 concentrations were made adjacent to each core location at approximately the same time as the core samples were collected. Gas-phase O_2 concentrations varied from atmospheric concentrations (20.9 vol%) at the tailings surface to ~10 vol% at a depth of 50 cm at most of the sample locations. Because the core samples were present in an oxic environment in situ, no special precautions were taken to isolate the samples from O_2 after collection.

3.2. Mineralogical study

The core samples were examined visually and >60 polished sections were made and examined under reflected light. Selected samples were also examined using SEM and

*1 t = 1 metric tonne = 10^3 kg.

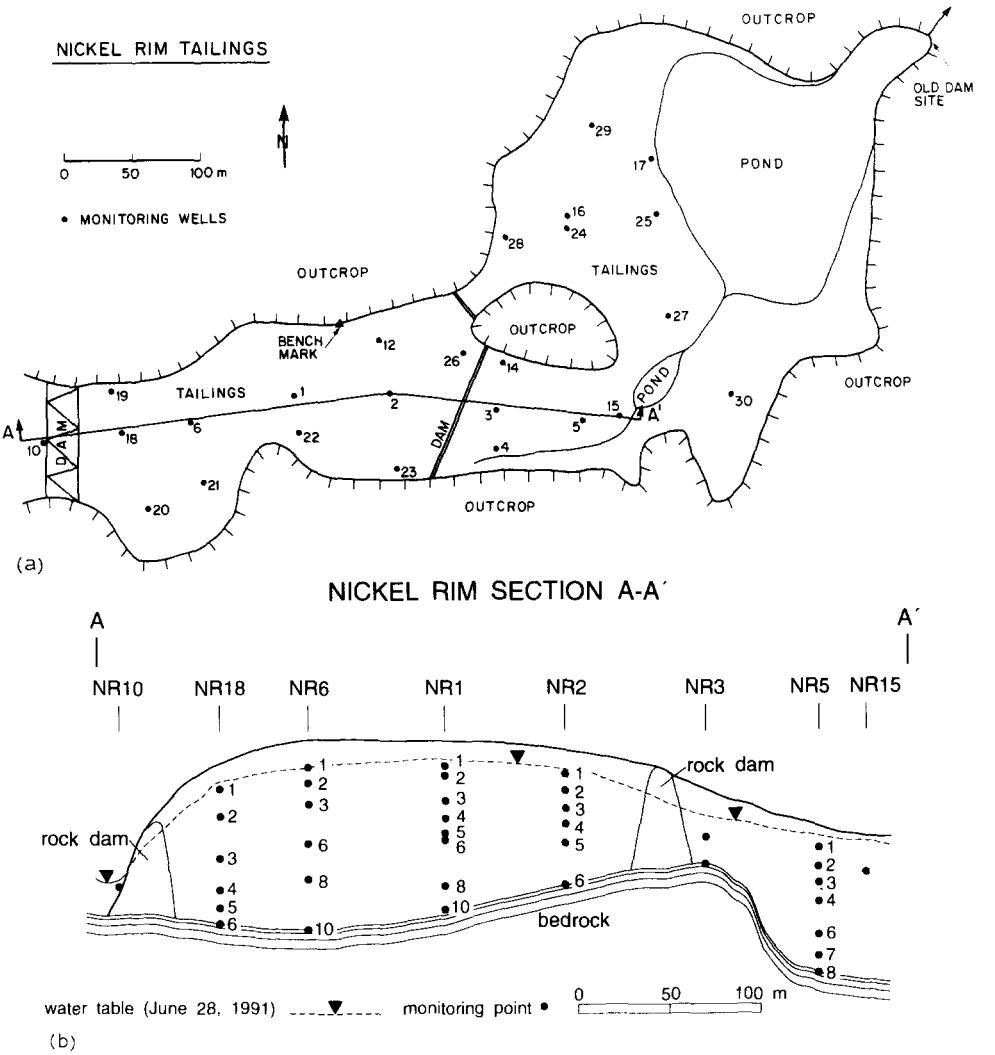

Fig. 4. (a) Area map and (b) cross-section along A–A' showing sample location at the Nickel Rim impoundment. Core samples from NR*1*, NR*2*, NR*6* and NR*18* were used for the chemical extractions. Core NR*1* was also used for the total rock analysis.

elemental analyses were conducted by EDXA. Additional elemental analyses were conducted using an electron microprobe. X-ray diffractometer patterns of bulk tailings samples were obtained for several locations, and the results were plotted vs. depth to determine the mineral-weathering sequence.

3.3. Chemical extractions

The tailings are composed of finely-ground gangue minerals, primarily silicates,

plus any unwanted or unrecoverable sulphide minerals. In the shallow part of the Nickel Rim tailings, oxidation has resulted in the replacement of the sulphide minerals. The results of the mineralogical study, described in detail below, indicate that the most abundant secondary minerals are the Fe-(oxy)hydroxides, primarily goethite, with lesser amounts of jarosite and gypsum. Johnson (1993) indicated that pH-buffering reactions depleted the carbonate mineral content of the tailings sampled to concentrations of <0.01 wt% as $CaCO_3$. As a result of these oxidation and neutralization reactions, three different fractions are expected to be found in the oxidized tailings: a water-soluble fraction (primarily gypsum); a reducible fraction (primarily jarosite and Fe-(oxy)hydroxides); and a residual fraction. Two steps were developed to extract these fractions.

The first fraction was extracted by adding 50 mL of deionized water to 1 g of tailings; the mixture was shaken continuously for 30 min at room temperature (step *1*: referred to as water-soluble fraction). The second fraction was extracted by heating the tailings sample in 30 mL of 2 *M* hydroxylamine hydrochloride ($NH_2OH \cdot HCl$) in 25% (v/v) acetic acid (HOAc) for 24 h at $95 \pm 4°C$ and with occasional agitation (step *2*: referred to as reducible fraction). For step *2* either residue from step *1* was used in the extraction, in which case the extraction is referred to as a sequential extraction, or a separate 1-g subsample of tailings was used directly. Following each treatment step, the extractants were filtered through cellulose acetate filters (0.45-μm filter size). Concentrated HCl was added to the step-*1* filtrate to lower the pH to <1. Blanks of the extraction solutions were analysed in the same manner as the other samples, and the metal concentrations in the extractions were adjusted to account for the reagent additions.

Determinations of total dissolved Ni, Cu, Cr, Mn, Zn, Pb, Co, Cd, Mg, Na, K, Ca and Al were performed with a flame-emission atomic absorption spectrophotometer (AAS). Total dissolved Fe was analysed by visible spectrophotometry using the Ferrozine® technique of Gibbs (1979). Total masses of metals in the tailings solids (referred to as total metal concentrations) were determined by Activation Laboratories Ltd., Ancaster, Ontario. Masses of the major elements Al, Fe_{total}, Mn, Mg, Ca and K were analysed by inductively coupled argon plasma emission spectrometry (ICP–AES) following a Li-metaborate fusion. Masses of Cu, Pb, Zn and Ni were determined by ICP–AES following a NO_3–HCl–$HClO_4$–HF digestion. Co and Cr were analysed by instrumental neutron activation analysis.

3.4. Choice of reagents and leaching conditions for extraction of the reducible fraction

The procedure used to extract the reducible fraction was adapted from step three of the procedure described by Tessier et al. (1979). At the field site, samples were in contact with gas-phase O_2, therefore oxygen was not excluded during the extraction procedure, which is contrary to the procedure of Tessier et al. (1985). As Tessier et al. (1989) recommended, the time of leaching and the reagent concentrations were modified to ensure that the Fe-oxide was completely extracted. Experiments were conducted to determine the conditions required for complete extraction of the Fe-(oxy)hydroxides, and to determine the optimal reagent volume, concentration,

Table 3
Parameters used for the extraction experiments, assessing the conditions required for complete dissolution of Fe-(oxy)hydroxides contained in 1 g of tailings

Experiment No.	Hydroxylamine hydrochloride		Acid[a]	Temperature (°C)	Time (h)
	volume (mL)	concentration (*M*)			
1	30	0.5	HOAc	95	3, 6, 8
2	40	0.5	HOAc	95	6
3	30	1	HOAc	95	3, 4, 5, 6, 9
4	30	0.14	HOAc	95	6
5	30	0.5	HOAc	25	6
6	30	2	HCl (1 *M*)	85	3, 4, 5, 7, 8, 10.5, 24, 25, 26
7	30	1	HOAc	85	6, 24, 25, 26
8	3 × 30	1	HOAc	85	6 + 5 + 11.5 (sequential)
9	30	2	HOAc	95	4, 5, 6, 7, 10, 15, 16, 17, 21, 23, 25, 39, 40, 41

[a] HOAc = acetic acid; HCl = hydrochloric acid.

temperature, leaching time and type of acid to add (HCl or HOAc) (Table 3). For these preliminary experiments, 1-g samples were taken from the same subsample of core NR*1*. These samples were subjected only to the reductive extraction step.

A comparison of nine extraction experiments (Fig. 5) shows that the rate of Fe release was strongly dependent on the temperature and concentration of $NH_2OH \cdot HCl$. The concentration of $NH_2OH \cdot HCl$ required for complete extraction was 2 *M*. This high concentration, four times that suggested by Tessier et al. (1989), was required because the tailings are rich in Fe-(oxy)hydroxides. Using HCl as the background acid, rather than HOAc, seemed to be more efficient. HOAc was used in

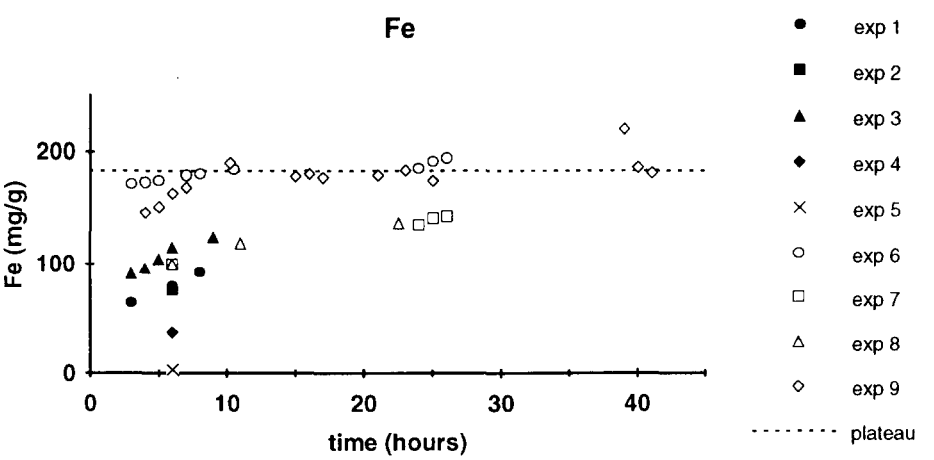

Fig. 5. Extraction of Fe vs. time. The parameters used for the nine experiments are given in Table 3. These experiments were conducted to determine the conditions required for the complete dissolution of the Fe-(oxy)hydroxides contained in the tailings.

the subsequent experiments because it was suspected that HCl would increase the potential for the dissolution of the silicate fraction. The results from these experiments suggest that, for the Nickel Rim tailings, extraction of reducible iron was complete after 24 h of leaching in a 2 *M* $NH_2OH \cdot HCl$ in 25% (v/v) HOAc solution at 95°C. These conditions were used for the remaining experiments.

The concentrations of several other metals, in addition to Fe, were determined for the same extractions. The results of these determinations (Fig. 6) give some indication of the efficiency of the method of extraction. Determinations of Ni, Cu, Cr, Co, Pb,

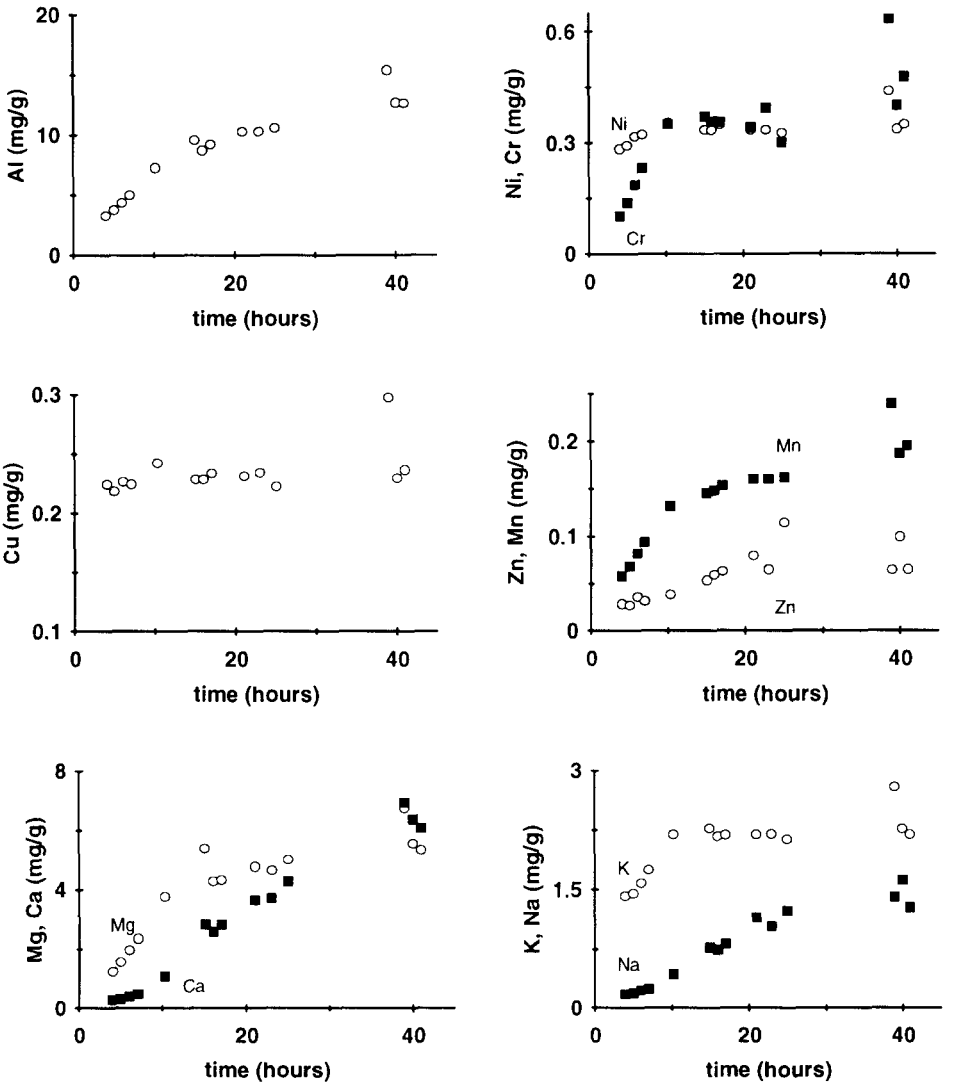

Fig. 6. Extraction of Al, Ni, Cr, Cu, Zn, Mn, Mg, Ca, K and Na vs. time. One-gram samples were digested for 24 h in 30 mL of 2 *M* hydroxylamine hydrochloride in 25% (v/v) acetic acid at 95°C.

Zn and K showed that constant concentrations were reached during the extraction by $NH_2OH \cdot HCl$ at about the same time as Fe. It was assumed, therefore, that all these metals were associated with the reducible-iron fraction. Al, Mg and Mn showed a slight increase continuing after a 24-h leaching time. The increase in Mn concentration may be attributed to the slower dissolution of crystalline Mn-oxides and -aluminosilicates following the dissolution of poorly-crystalline Fe(III)- and Mn-(oxy)hydroxides. Consequently, the Mn concentration obtained after a 24-h leaching time was assumed to represent the amount of Mn available to reductive dissolution. Similarly, an observed slight increase in Al and Mg concentrations between 24 and 40 h may be the result of the slow dissolution of aluminosilicates following the release of Al and Mg associated with the Fe-(oxy)hydroxides.

Lastly, Ca and Na concentrations did not reach any constant value during the leaching period. It was therefore not possible to know which part of the extracted Ca and Na could be associated with the reducible fraction. Comparison of the extracted Ca and Na concentrations with the mass of the residual fraction, however, showed that only a small fraction of these two elements was extracted. It is reasonable, therefore, to assume that even if the reductive step is not completely selective, the mass of residual fraction attacked by the $NH_2OH \cdot HCl$ solution is not large enough to affect the overall results. The concentration of Cd was consistently below the detection limit, and was not analysed further.

3.5. Comparison between water-soluble and reducible extractions

A comparison was made to assess the concentrations of metals extracted by water and those extracted using the strongly reducing solution (Table 4). This comparison was made for six 1-g tailings samples from the same subsample of core NR*1*; three were subjected to the water-dissolution step only, and three were subjected to the reductive step only. The results, presented as the mean of the three replicates for each step and for each metal, suggest the mass of metals removed by the water-dissolution step is much less than the mass removed by the reductive step. Because metals released in the water-soluble fraction will also be susceptible to release under the conditions used to extract the reducible fraction, extractions using the reductive step only are probably representative of the total masses of metals potentially available for release under an organic-rich cover. Therefore, core samples collected from three additional locations (NR*2*, NR*6* and NR*18*) were subjected only to the reductive step of the extraction procedure.

3.6. Precision and accuracy of the results

The precision and accuracy of the experimental results were assessed by analysing three replicates of each of the upper eight subsamples of the core NR*1*. For each of these subsamples, three 1-g samples were subjected to the sequential extraction. As three values were insufficient to obtain a reliable standard deviation, it was assumed that for each metal the standard deviation was the same for each series of three

Table 4
Concentrations of extracted metals relative to total metal concentrations (all concentrations expressed in mg/g tailings)

	Concentration of metals													
	Fe	Ni	Cu	Zn	Co	Mn	Cr	Pb	Cd	Ca	Mg	K	Na	Al
Total	184	0.48	0.33	0.15	0.025	1.39	0.50	0.005	–	47.3	41.0	4.82	14.0	46.5
Extractable:														
water step	0	0	0.002	0	0	0.001	0	0	0	0.078	0.049	0.006	0.014	0
% of total	0	0	0.61	0	0	0.07	0	0	0	0.16	0.12	0.12	0.10	0
$NH_2OH \cdot HCl$/ HOAc step	198	0.28	0.15	0.033	0.024	0.15	0.31	0.041	0	3.80	4.36	2.60	1.03	9.56
% of total	108	57.8	45.5	21.4	96.0	10.8	62.0	–	–	8.03	10.6	54.0	7.38	20.6

samples, and was equal to the standard deviation for all the samples. This assumption was tested by using the statistical test of the ratio of two variances and the F distribution. The null hypothesis, that the variance of the replicates from the same subsample is not significantly different from the variance of all the samples, was discredited for only a few cases. No metal, at any depth, showed a variance that was significantly different from the overall variance for that metal. The results of the statistical analysis (Fig. 7) showed that the variations in concentration vs. depth are greater than the variations between the three samples from the same depth, with the exception of Zn and Ca.

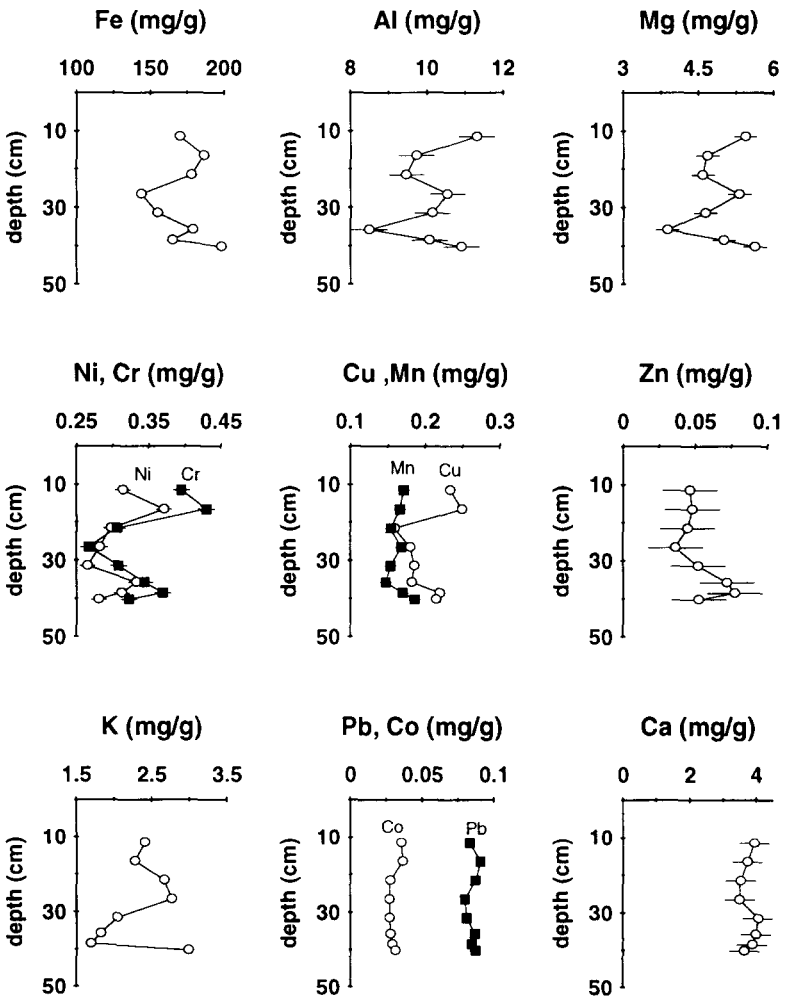

Fig. 7. Depth vs. masses of Fe, Al, Mg, Ni, Cr, Cu, Mn, Zn, K, Pb, Co and Ca extracted during the reductive step. Each value has been obtained from the mean of three replicates. The *bar* on each plot represents twice the standard deviation.

4. Results of the mineralogical study

The mineralogical study indicated that the samples could be divided into primary minerals, secondary minerals and tertiary minerals. Primary minerals are those that constituted the ore and gangue assemblages. Secondary minerals are those that originate in the tailings impoundment. With the exception of gypsum, which may precipitate directly from the mill-discharge water, secondary minerals originate from the reprecipitation of dissolved constituents derived from sulphide-mineral oxidation reactions or mineral-dissolution reactions. Tertiary minerals are those that form after the tailings samples have been removed from the impoundment. In general, it was possible to distinguish primary, secondary and tertiary minerals during the mineralogical study (Table 5).

Table 5
Mineralogy of Nickel Rim tailings

Primary	Secondary	Tertiary
Major (>10%):		
Magnesiohornblende–actinolite	jarosite	gypsum
Calcic plagioclase	goethite	covellite
Augite	gypsum	ferrihydrite
Magnetite	vermiculite	lepidocrocite
Pyrrhotite		rozenite
		siderotil
Minor (1–10%):		
Chlorite	ferrihydrite	
Biotite	sulphur	
Talc	covellite	
Quartz		
Enstatite		
Trace (<1%):		
Pentlandite		
Pyrite		
Chalcopyrite		
Marcasite		
Albite		
Ilmenite		
Muscovite		
Also detected:		
Rutile		
Hercynite		
Ülvospinel		
Tremolite		
Epidote		
Hematite		

4.1. Primary minerals

4.1.1. Primary sulphides

Optical microscopy showed that pyrrhotite is the principal sulphide, making up >98% of the sulphide fraction (Fig. 8). X-ray diffractograms of hand magnetic concentrates indicate that both monoclinic and hexagonal pyrrhotite are present, but that the monoclinic form is more abundant. Most, but not all, of the pyrrhotite grains are Ni-bearing. Energy-dispersion analyses indicate that the Ni content is generally ~1 wt%.

The remaining sulphides are predominantly chalcopyrite, pentlandite, pyrite and marcasite. The relative abundance of the minor sulphides in the tailings is estimated to be chalcopyrite > pentlandite > nickeliferous pyrite > marcasite. Pyrite and marcasite are not quantitatively significant. Although the pyrite in the tailings is generally Ni-rich, values obtained by energy-dispersion analyses are highly variable, ranging from 0 to ~7 wt%.

4.1.2. Principal silicate minerals

Minerals in the silicate fraction of the tailings were determined by optical microscopy and X-ray diffractograms, supplemented by heavy-liquid and Frantz® isodynamic magnetic separations, by Debye–Scherrer X-ray patterns, and by SEM and microprobe analyses (Jambor and Owens, 1993). The principal components of the tailings are calcic plagioclase and amphibole that are accompanied by substantial amounts of clinopyroxene, chlorite, biotite, talc, quartz and magnetite (Table 5).

Fig. 8. Backscattered-electron (BSE) photo of three large grains of unaltered pyrrhotite, one pure, one containing inclusions of pyrite (*py*, dark) and pentlandite (*pn*, light), and the third containing laths of marcasite. Accompanying grains are ilmenite (*il*) and magnetite (*mag*). The pyrite and marcasite are nickeliferous (~2–3 wt% Ni). *Bar scale* represents 25 μm.

Table 6
Microprobe analyses (in wt%) of amphibole in Nickel Rim tailings

	Grain *1*	Grain *2*	Grain *3*	Grain *4*	Grain *5*
Na_2O	0.5	0.1	0.8	0.5	0.1
K_2O	0.2	0.5	0.2	0.2	0.0
CaO	11.9	11.3	12.2	13.7	11.9
MgO	15.9	15.6	14.3	14.4	14.3
FeO	14.0	14.2	15.6	14.7	17.0
MnO	0.1	0.3	0.1	0.3	0.3
TiO_2	0.3	0.0	0.5	0.5	0.0
Al_2O_3	4.0	2.1	3.8	2.8	1.7
SiO_2	50.9	54.6	50.3	51.1	52.4
Cl	0.2	0.0	0.3	0.3	0.0
Sum	98.0	98.7	98.1	98.5	97.7

Most of the plagioclase is calcic, i.e. of intermediate composition in the albite–anorthite series, but albite is also common. The X-ray pattern for the bulk of the amphibole fits well with data for magnesiohornblende (PDF *20-481*); microprobe analyses of hand-picked grains from sample NR*18-35* gave compositions that, although close to magnesiohornblende, lie within the fields of actinolitic hornblende and actinolite (Table 6). It is probable, however, that the hornblende rarely falls outside the compositional range actinolite–magnesiohornblende. Augite is a major constituent of the tailings; enstatite is also common, but is much less abundant than augite. Biotite formula contents of Mg are generally in the range $Mg_{55}Fe_{45}$ to $Mg_{65}Fe_{35}$, thus, depending on which compositional definition is used, the mineral could be called phlogopite. Transmitted-light microscopic examination of the tailings showed that much of the chlorite and all of the talc occur as fine-grained replacements and pseudomorphs of pyroxene and amphibole.

4.2. Secondary minerals

Goethite, K-dominant jarosite and gypsum are the principal minerals that precipitated in situ. Goethite and jarosite are confined to the oxidation zone, are abundant in it, and give the tailings a rusty, ochreous appearance. The precipitation of goethite, jarosite and gypsum fills the voids of the tailings and thereby cements the tailings. Precipitation of these minerals has been locally sufficient to cement the tailings into hardpan layers, 10–15 cm thick, which are difficult to penetrate with a soil auger or shovel. Measurements of gas-phase O_2, N_2 and CO_2 concentrations suggest that these layers affect the movement of pore gases through the tailings (Johnson, 1993).

The minor to trace secondary minerals are ferrihydrite, sulphur and covellite. Of these, sulphur is the most abundant. It occurs always as a partial replacement of pyrrhotite, and is usually present only where some residual pyrrhotite remains. Ferrihydrite occurs in only trace amounts, and covellite is found only near the border

between the oxidized and unoxidized tailings. Covellite is found typically at the edge of pyrrhotite grains.

5. Results of the chemical extraction procedure

5.1. Water-soluble fraction

The water-soluble fraction contains metals derived from the redissolution of tertiary phases, which accumulated during core drying and evaporation of the pore water, metals derived from the redissolution of water-soluble primary or secondary phases such as gypsum ($CaSO_4 \cdot 2H_2O$), or metals that desorbed from sulphide, (oxy)hydroxide, or other surfaces. It is possible, as noted by Nirel and Morel (1990), that a portion of the metals released through the dissolution could be readsorbed onto other phases present in the tailings. No effort was made to quantify concentrations of adsorbed metals. The estimate of the metal masses released through the water-extraction step may, therefore, be low.

5.1.1. Iron, aluminium

The Fe concentration in the water-soluble fraction increases sharply at 35 cm in core NR*1* (Fig. 9), rising from the detection limit (0.005 mg g^{-1}) to 0.2 mg g^{-1}. Geochemical data from the tailings pore water indicate that Fe concentrations

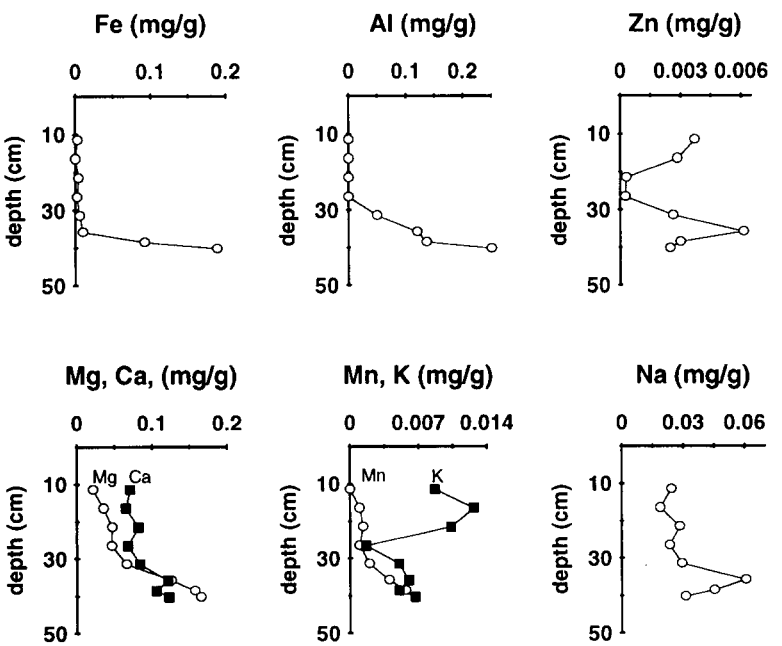

Fig. 9. Concentrations of Fe, Al, Zn, Mg, Ca, Mn, K and Na vs. depth in the water-soluble fraction of core NR*1*. Concentrations of Ni, Cu, Cr, Co and Pb are below analytical detection limits.

increase sharply at ~30 cm and that high dissolved concentrations persist throughout the upper 2 m of the tailings (Johnson, 1993). Al shows a pattern similar to that of Fe, with a sharp increase at a depth of 30 cm, from the detection limit (0.1 mg g^{-1}) to 0.25 mg g^{-1}. Concentrations of dissolved Al increase from <0.1 mg L^{-1} at a depth of 30 cm, to 900 mg L^{-1} at a depth of 150 cm (Johnson, 1993). These observations indicate that Fe and Al contained in the water-soluble fractions are probably derived from redissolution of Fe(II) and Al tertiary precipitates formed by evaporation of tailings pore water during sample preparation.

5.1.2. Manganese, magnesium, calcium

Mn, Mg and Ca show a smoother increase in concentration than Fe or Al. Manganese ranges from the detection limit (0.002 mg g^{-1}) to 0.007 mg g^{-1} (Fig. 9). Mg ranges from the detection limit (0.002 mg g^{-1}) to 0.18 mg g^{-1}. The concentration of Ca ranges from 0.065 to 0.13 mg g^{-1} (detection limit is 0.005 mg g^{-1}). The mass of Ca is in excess of that expected to be released by the redissolution of precipitates accumulated during drying, suggesting that some Ca is released by the dissolution of secondary gypsum ($CaSO_4 \cdot 2H_2O$).

5.1.3. Zinc, sodium, potassium

Concentrations of Zn, Na and K in the water-soluble fraction do not show a consistent pattern and are very low in the upper 40 cm (Fig. 9). Zn concentrations range from the detection limit (0.002 mg g^{-1}) to 0.0065 mg g^{-1}, Na concentrations range from 0.015 to 0.062 mg g^{-1} (detection limit is 0.001 mg g^{-1}) and K concentrations range from the detection limit (0.001 mg g^{-1}) to 0.013 mg g^{-1}.

5.1.4. Nickel, copper, cobalt, lead

Ni, Cu, Co and Pb are below their detection limits (0.005 mg g^{-1} for Ni, Cu and Co; 0.05 mg g^{-1} for Pb).

5.2. Reducible fraction

The results of the mineralogical study indicate that Fe-(oxy)hydroxides and jarosite are abundant in the upper 120 cm of the tailings at location NR*1*. Goethite is the most abundant of these Fe-(oxy)hydroxides. The fraction of tailings susceptible to reduction is composed principally of Fe-(oxy)hydroxides, for example goethite (α-FeOOH) or ferrihydrite ($Fe(OH)_3$), precipitated after the release of Fe^{2+} by sulphide oxidation through the reactions:

$$Fe^{2+} + \tfrac{1}{4}O_2 + \tfrac{3}{2}H_2O \rightleftharpoons FeOOH + 2H^+ \quad (1)$$

or

$$Fe^{2+} + \tfrac{1}{4}O_2 + \tfrac{5}{2}H_2O \rightleftharpoons Fe(OH)_3 + 2H^+ \quad (2)$$

This fraction also contains jarosite precipitated through the reaction:

$$FeS_2 + \tfrac{5}{2}H_2O + \tfrac{15}{4}O_2 + \tfrac{1}{3}K^+ \rightarrow \tfrac{1}{3}KFe_3(SO_4)_2(OH)_6 + \tfrac{4}{3}SO_4^{2-} + 3H^+ \quad (3)$$

For NR*1* core samples above 40 cm subjected to both extraction steps, metal concentrations in the water-soluble fraction were much lower than those in the reducible fraction (Table 4). Therefore, additional samples were subjected only to a single reductive step due to the likelihood of insignificant contributions by the water-soluble extraction procedure. The following results (Figs. 10–13) are presented, therefore, as either the sum of the values obtained for the water-soluble and reductive steps for the samples subjected to the sequential extraction (upper portion of core NR*1*), or, the value obtained by using the single reductive step for the remaining samples. Both of these values are referred to as "total extractable metal contents".

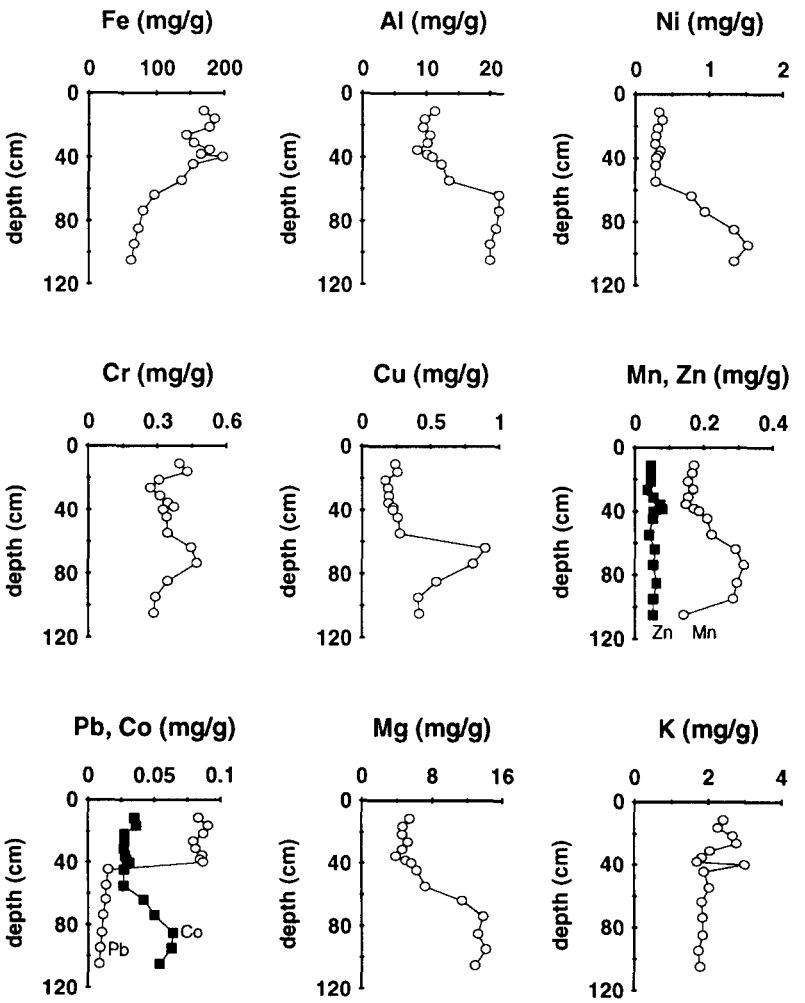

Fig. 10. Total extractable concentrations of Fe, Al, Ni, Cr, Cu, Mn, Zn, Pb, Co, Mg and K vs. depth for core NR*1*. The amounts of metals are the sum of the water-soluble fraction and the reducible fraction when both steps were completed sequentially. When the reductive step only was performed, the result is considered to represent the total extractable metal content.

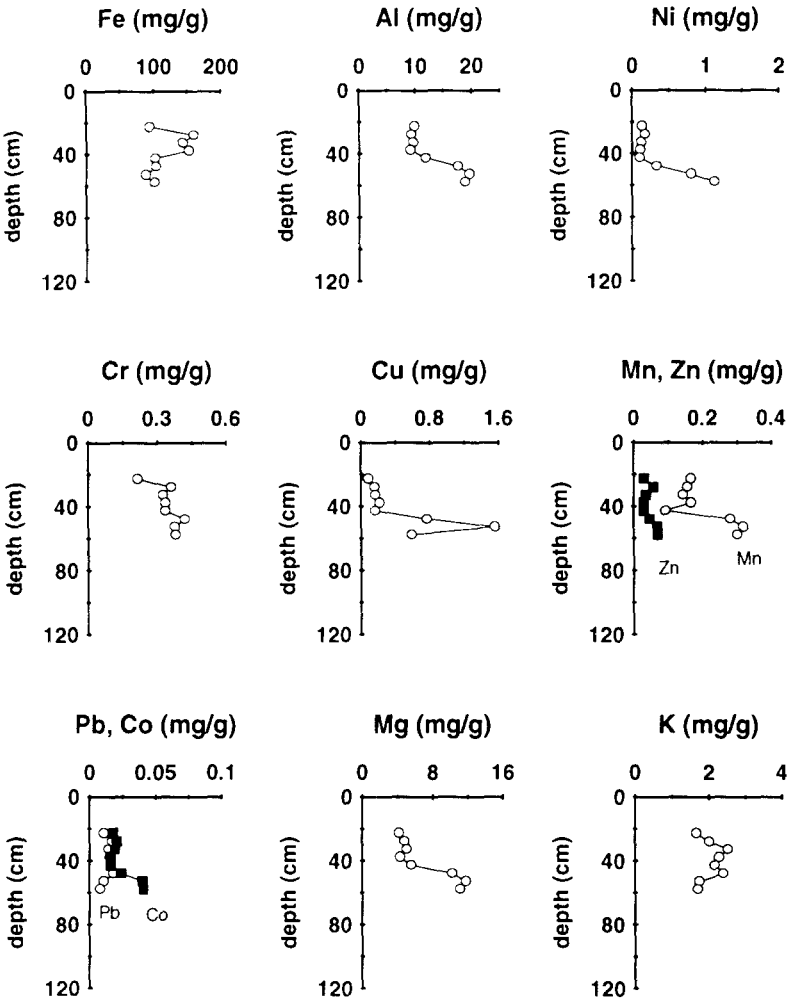

Fig. 11. Total extractable concentrations of Fe, Al, Ni, Cr, Cu, Mn, Zn, Pb, Co, Mg and K vs. depth for core NR*2* measured using the reductive step only.

The four cores NR*1*, NR*2*, NR*6* and NR*18* can be divided into two categories: NR*1* and NR*2*, which were divided into subsamples according to physical observations; and NR*6* and NR*18*, which were evenly cut into 10-cm-long samples. As a consequence, for cores NR*6* and NR*18*, depths with high concentrations of metals may have been mixed with depths with low concentrations. This mixing lessens the magnitude of the variations in concentration vs. depth, but it gives a more general idea of the variations in concentration through the cores. On the other hand, NR*1* and NR*2* present a more pronounced pattern and therefore reveal subtle details about variations in concentration vs. depth (Figs. 10–13).

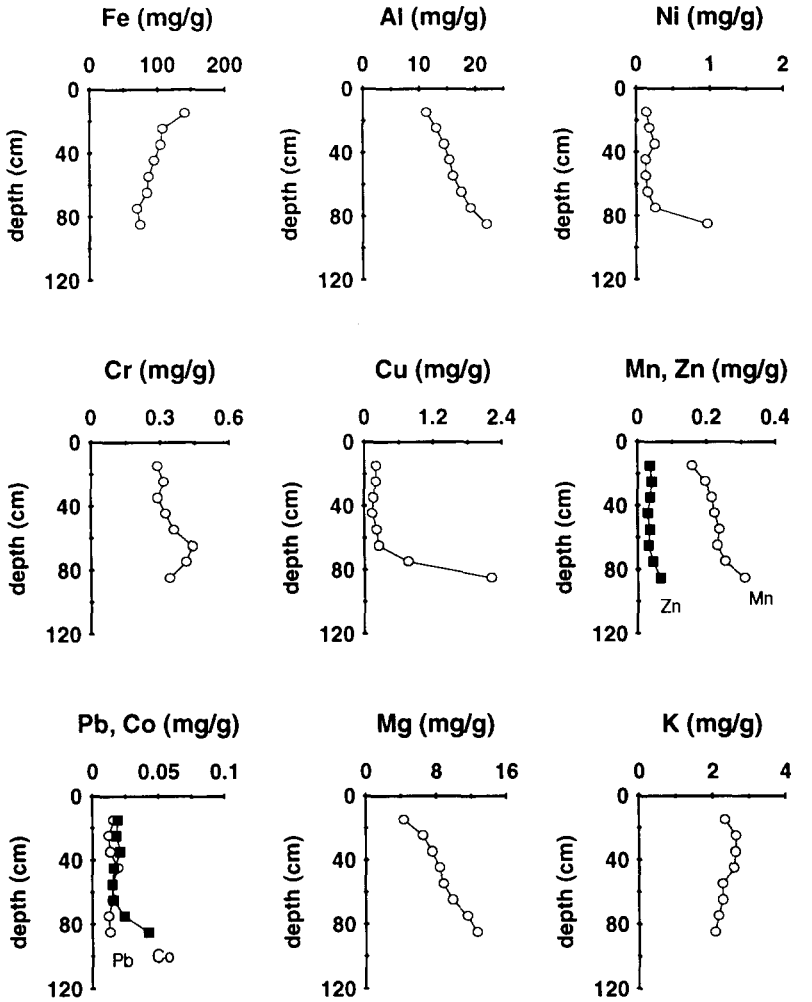

Fig. 12. Total extractable concentrations of Fe, Al, Ni, Cr, Cu, Mn, Zn, Pb, Co, Mg and K vs. depth for core NR6 measured using the reductive step only.

5.2.1. Iron

The Fe concentrations decrease from the upper part of the tailings, where concentrations are as high as 200 mg g^{-1}, to the partly-oxidized and then non-oxidized zones (Figs. 10–13). This decrease is particularly evident for core NR6. The high Fe concentrations near the tailings surface result from the more intensive sulphide oxidation processes occurring in the upper part of the tailings. The results of the mineralogical study indicate that pyrrhotite is almost completely obliterated in the shallowest core samples (Fig. 14), where the extractable Fe concentrations are generally the greatest. In this zone, replacement of pyrrhotite by goethite, elemental sulphur and jarosite has been extensive. Below this zone, replacement of pyrrhotite has been less extensive, corresponding to lower concentrations of extractable Fe. At a

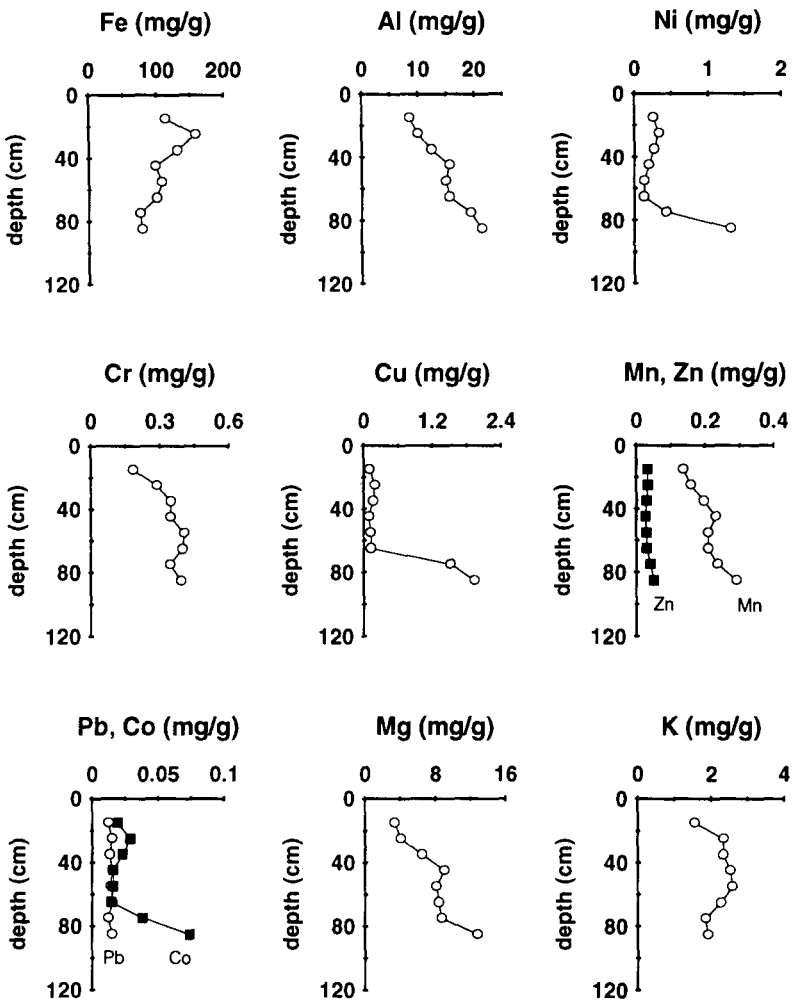

Fig. 13. Total extractable concentrations of Fe, Al, Ni, Cr, Cu, Mn, Zn, Pb, Co, Mg and K vs. depth for core NR*18* measured using the reductive step only.

more detailed scale, a hardpan layer, rich in Fe-oxides, is indicated by a local increase in the Fe concentration at ~40-cm depth especially in core samples NR*1* and NR*2*. This increase in extractable Fe concentration corresponds closely to visual observations and mineralogical analyses of the tailings, which indicate that the tailings at this depth are cemented by secondary precipitates, dominated by jarosite, goethite and gypsum.

5.2.2. Nickel

Ni was extracted from the Nickel Rim ore, and relatively high residual concentrations of Ni occur (0.1–1.5 mg g^{-1} of tailings) in the form of pentlandite and nickeliferous pyrite in the unoxidized zone of the tailings. Incorporation of Ni in

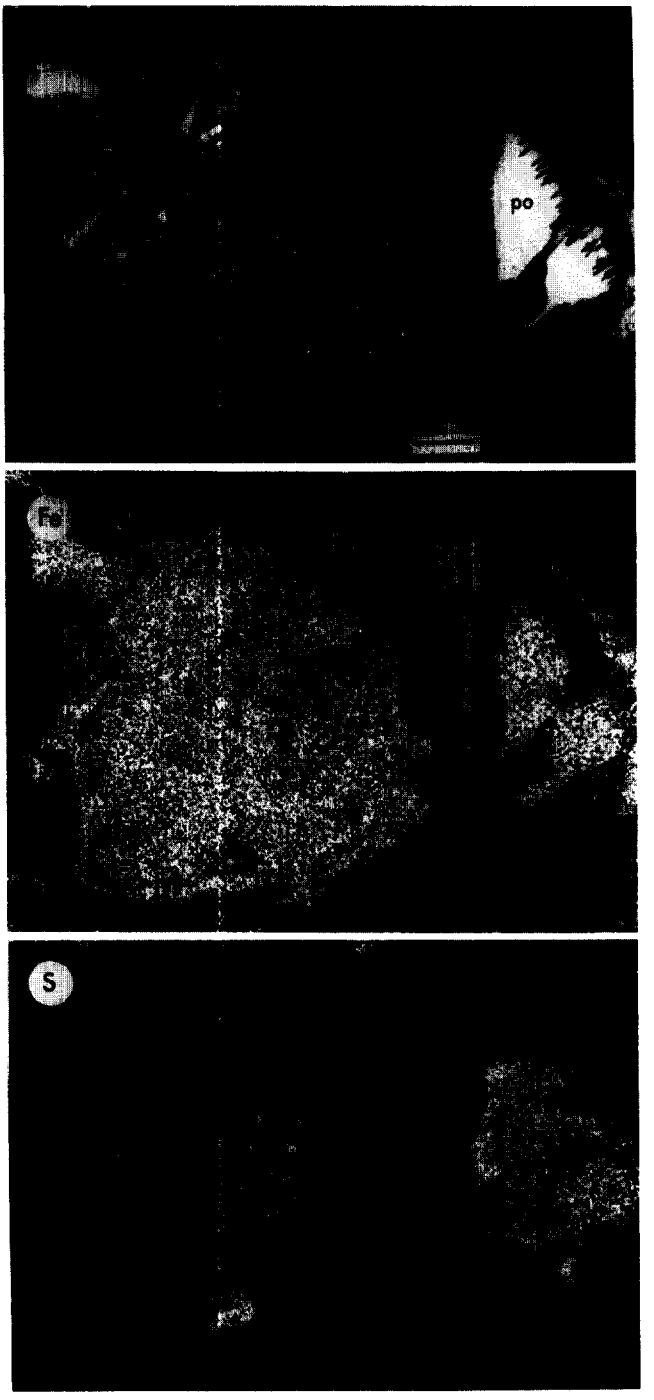
po
Fe
S

sulphide oxidation products, therefore, was expected to occur. Concentrations of extractable Ni obtained for the upper, intensely oxidized zone of the tailings (upper 60 cm) range from 0.1 to 0.45 mg g^{-1}. Microprobe analyses indicate that goethite is locally Ni-bearing (Fig. 15). It is likely, therefore, that adsorption or coprecipitation with goethite is probably the dominant solid-phase control on dissolved Ni concentrations in the oxidized zone of the tailings, and that the extractable Ni concentrations primarily represent this Ni incorporated in goethite. The Ni concentrations increase slightly at the hardpan level, and then rise sharply in the deeper cores, corresponding to the partly oxidized tailings. This last increase may be due to the partial dissolution of Ni-bearing sulphide minerals by the acidic $NH_2OH \cdot HCl$/HOAc solution. Alternatively, the increase may indicate greater accumulations of Ni within Fe(III)-(oxy)hydroxide minerals at and below the cemented layer.

5.2.3. Chromium

In the upper part of the tailings, where no sulphide minerals are present, the concentration and behaviour of Cr are very similar to the concentration and behaviour of Ni. Concentrations of Cr increase slightly at the hardpan level, but remain relatively constant at other depths. Concentrations of Cr vary from ~0.2 to ~0.5 mg g^{-1}, which is slightly greater than the concentrations of Ni. The results of the mineralogical study indicate that Cr is contained in magnetite, and in the alteration rims that surround magnetite grains (Fig. 16). Microprobe analysis of an isolated magnetite grain indicated that the magnetite contains 6.9% Cr_2O_3 and that the alteration product contains 13.2% Cr_2O_3 (Table 7). Magnetite is a mixed-valence Fe mineral. Decomposition of this Cr-rich magnetite by the reduction procedure may have contributed Cr, in addition to the Cr released by the decomposition of Cr-rich alteration products.

5.2.4. Copper

The concentrations of Cu range from 0.1 to 2.2 mg g^{-1}. The mineralogical study indicates that the partly-oxidized zone contains abundant covellite (CuS). The results obtained by the reductive step of the extraction procedure indicate that Cu concentration increases sharply within a limited zone that corresponds with the depth of the covellite-bearing zone. Covellite is a secondary Cu-sulphide that may be susceptible to reductive dissolution. Consequently, the actual concentration of Cu associated with Fe-oxides is estimated to vary from 0.1 to 0.35 mg g^{-1}, which is the range of variation of the Cu concentrations in the upper 60 cm of the tailings. As for Ni and Cr, a slight increase in concentration is observed at the hardpan level.

5.2.5. Manganese

Concentrations of Mn vary between 0.14 and 0.32 mg g^{-1} and show a slight, but

Fig. 14. BSE photo of goethite (*go*) pseudomorphous after pyrrhotite. Grain at right consists of residual pyrrhotite (*po*) enclosed in sulphur, in turn surrounded by a relatively thin rim of goethite. Accompanying silicates are intergrown albite and augite (*cpx*), and amphibole (*am*). Beneath the BSE photo, X-ray maps for Fe and S outline the areas of goethite and sulphur, respectively. *Bar scale* represents 25 μm.

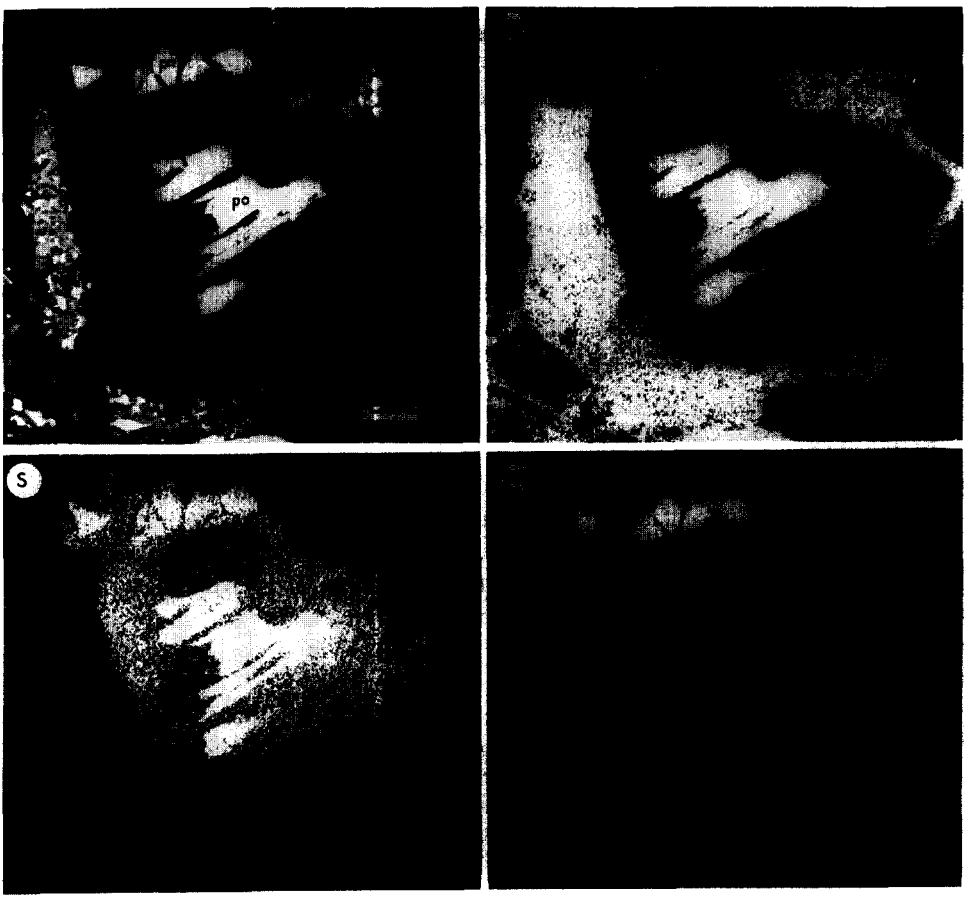

Fig. 15. Relict core of pyrrhotite (*po*) encompassed within a void (black) that was probably sulphur, with an outermost rim of goethite (*go*) in two shades: the outer, lighter portion contains slightly more S, Al, and Si than does the inner. X-ray maps for Fe, S and Ni show the distributions of these elements. The map for S shows the sulphur-rich character of the central void, and the map for Ni shows the presence of pentlandite (*pn*, top) and the slightly nickeliferous compositions of the pyrrhotite. *Bar scale* represents 25 μm.

constant increase with depth. The results of the mineralogical study indicate that Mn is contained in the pyroxenes and amphiboles of the silicate portion of the tailings (Tables 6 and 8). These silicate minerals have been altered in the oxidized zone of the tailings. It is probable that some of the residual Mn is retained in the Fe-(oxy)hydroxide precipitates. It is unlikely that Mn is derived from carbonate minerals, which probably were consumed previously by pH-buffering reactions.

5.2.6. Zinc, lead, cobalt

The $NH_2OH \cdot HCl$ solution was contaminated with respect to Zn, and a large variance was observed for this element. This factor makes it difficult to identify any pattern in the distribution of Zn vs. depth. In addition, the Zn concentration is about

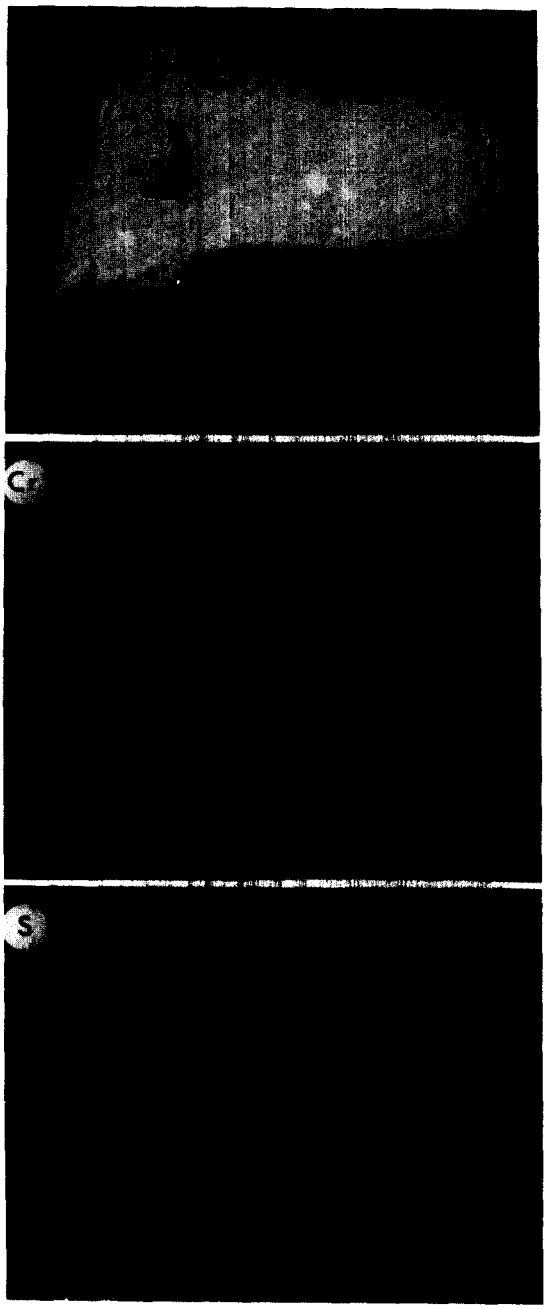

Fig. 16. BSE photo of altered grain of chromian magnetite. Note the alteration along the rim, but also penetration at the top and left interior; replacement is by Cr- and S-bearing Fe-oxyhydroxide (probably goethite, but the abundant shrinkage cracks are texturally characteristic of ferrihydrite). X-ray maps show a slight concentration of Cr at the alteration interface, and increased sulphur in the goethite rim. *Bar scale* represents 10 μm.

Table 7
Microprobe analyses of magnetise and associated alteration[a]

Magnetite*				Alteration*	
	(wt%)	ratio[b]			(wt%)
FeO	31.1	Fe	0.98	Fe_2O_3	27.6
ZnO	0.6	Zn	0.02	ZnO	1.4
Fe_2O_3	54.5	Fe	1.55	TiO_2	16.8
Cr_2O_3	6.9	Cr	0.20	Cr_2O_3	13.2
TiO_2	5.2	Ti	0.15	Al_2O_3	5.9
Al_2O_3	2.3	Al	0.10	S[c]	1.2
Total	100.6				66.1

[a] Sample from oxidation zone of core NR2, depth 32–36 cm.
[b] Formula ratio for four oxygen atoms.
[c] Wavelength peak position is in accordance with sulphide-sulphur rather than sulphate.

one order of magnitude lower (~0.04 mg g^{-1}) than that of the previously-discussed metals. Difficulties were also encountered with the analysis of Pb because of contamination. The concentrations of Pb vary less than those of Zn, and show no particular pattern vs. depth. The Co concentration is also very low, varying between 0.02 and 0.04 mg g^{-1}. For all four core sites, the behaviour of Co seems to be similar to the behaviour of Ni, particularly in the partly oxidized zone; a sharp increase takes place at a depth of 90 cm, suggesting a relation with the sulphide minerals.

Table 8
Microprobe analyses of pyroxenes in Nickel Rim tailings

	1	*2*	*3*
	Augite	Enstatite	Augite[a]
Location	NR2	NR2	NR18
Depth (cm)	32–36	32–36	50–100
CaO	19.7	2.4	23.5
MgO	15.3	26.7	12.0
FeO	10.5	17.8	9.0
MnO	0.4	0.4	–
TiO_2	0.5	0.3	0.8
Al_2O_3	1.7	1.1	2.9
SiO_2	50.7	51.8	51.8
Total	98.8	100.5	100.0

Formula for six oxygen atoms:
1:augite, $(Ca_{0.80}Mg_{0.20})_{\Sigma 1.00}(Mg_{0.66}Fe_{0.34}Ti_{0.01}Mn_{0.01})_{\Sigma 1.02}(Si_{1.92}Al_{0.07})_{\Sigma 1.99}O_{6.00}$.
2: enstatite, $(Mg_{1.46}Fe_{0.54}Ca_{0.09}Mn_{0.01}Ti_{0.01})_{\Sigma 2.11}(Si_{1.90}Al_{0.05})_{\Sigma 1.95}O_{6.00}$.
3: augite, $Ca_{0.94}(Mg_{0.67}Fe_{0.28}Ti_{0.02})_{\Sigma 0.97}(Si_{1.94}Al_{0.13})_{\Sigma 2.07}O_{6.00}$.
[a] Semi-quantitative data.

5.2.7. Aluminium, magnesium, potassium

Al has the second highest concentration after Fe and varies from ~10 to ~20 mg g^{-1}. For NR*1* and NR*2*, this concentration changes abruptly between 40- and 50-cm depth, from ~10 mg g^{-1} in the upper part to ~20 mg g^{-1} in the lower part. For NR*6* and NR*18*, the change in concentration is more gradual. In the upper part of NR*1*, where more detail is available, Al seems to behave differently than most other metals. Al probably is released initially to the pore water by aluminosilicate dissolution in the low-pH zone near the tailings surface. As neutralization reactions occur deeper in the tailings, formation of Al- hydroxide or basic Al-sulphate solids, or coprecipitation of Al with Fe(III)-(oxy)hydroxide solids, is favoured, likely leading to the increased concentrations of solid-phase Al observed in the tailings. The mineralogical study indicates that aluminosilicate minerals, particularly biotite, have been extensively altered, leading to the depletion of Al in the near-surface zone of the tailings.

Concentrations of Mg vary in a manner similar to Al, ranging from 3 to 14 mg g^{-1} tailings, with a very abrupt increase between these two values for both NR*1* and NR*2*. The concentration of K ranges from 1.5 to 2.5 mg g^{-1} and is relatively constant vs. depth, without any particular pattern. No striking differences between the four cores were noted.

5.3. Comparison with whole-rock analysis

The results of a whole-rock analysis of core NR*1* are shown in Fig. 17. Area plots (Fig. 18) and tabulated data (Table 4) aid in the comparison of the metal content of the reducible fraction and the total metal content. The results suggest that, in the shallow tailings, Fe was totally recovered by the sequential extraction. Cr was also extracted completely. Ni, Cu and Co were almost recovered completely in the upper 50 or 60 cm, which are the well-oxidized zone of the tailings. In the lower, less-oxidized zone, the recovery of these elements was partial, and it is likely that Ni, Cu and Co are associated with sulphide minerals that were partly digested by the reductant solution. Pb was recovered completely. Between 20% and 50% of the Zn was extracted, but only small fractions of Mn, Al, Mg and K were recovered. The remaining amounts are assumed to be associated with aluminosilicate minerals.

6. Implications

Mineralogical study indicates that the dominant Fe-(oxy)hydroxide mineral in the oxidized zone of the tailings is goethite. Fe, Ni and Co are contained in this goethite. Cr is contained in magnetite derived from the orebody and from the alteration rims which surround the primary magnetite grains. Cu is probably present as the secondary sulphide mineral covellite. The location of Pb is unconfirmed, but is assumed to be within the Fe-(oxy)hydroxide precipitates.

In the upper part of the tailings, at least six metals (Fe, Ni, Co, Cr, Cu and Pb) were completely extracted by $NH_2OH \cdot HCl$. These results suggest that large masses of Ni,

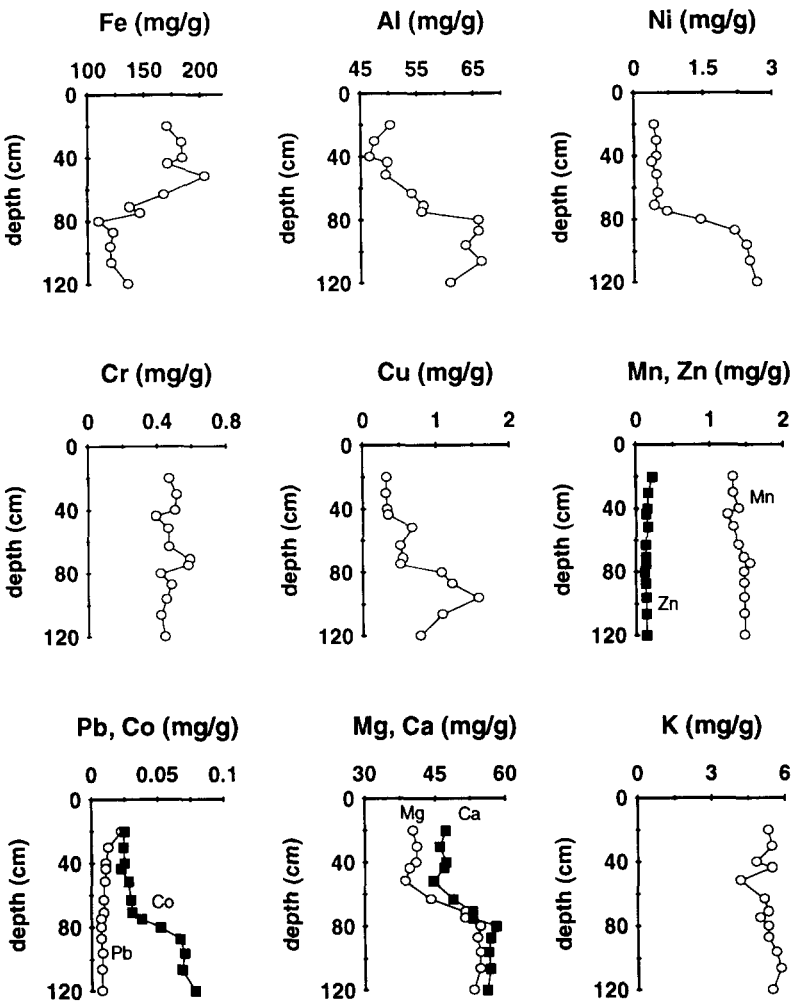

Fig. 17. Whole-rock analysis of core NR*1*: concentrations of Fe, Al, Ni, Cr, Cu, Mn, Zn, Pb, Co, Mg, Ca and K vs. depth.

Cr, Co and Pb are contained in the Fe-(oxy)hydroxides of the upper 40–60 cm of the tailings, and that these metals potentially are available for release by reductive dissolution.

The total mass of metals contained in the western portion of the impoundment can be estimated by assuming that the volume of the tailings is a parallelepiped as shown in Fig. 19. Assuming also that concentrations at the four relevant core sites can be represented by the mean of the analysed values for the first 60 cm, then the concentration $c(x)$ on each point on the x-axis can be linearly interpolated from the concentration of NR*1*, NR*2*, NR*6* and NR*18*. If the concentration on each point of the y-axis is equal to the concentration for $y = 0$, and the average bulk density ρ_b of the tailings is constant and equal to 1.58 g cm^{-3} (Johnson, 1993), the masses of metals

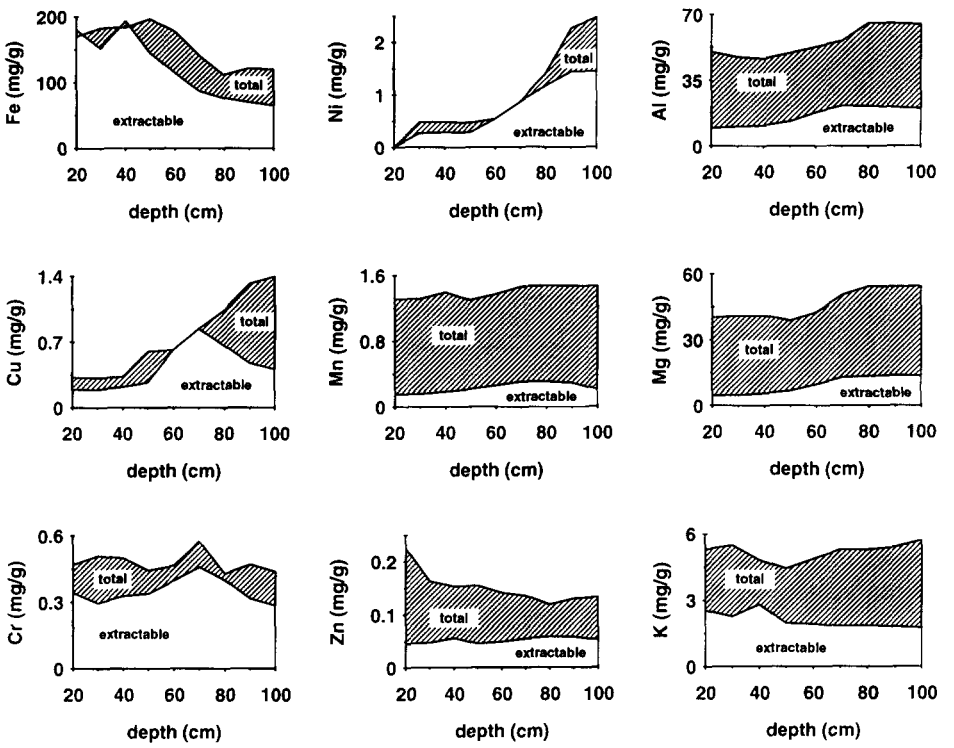

Fig. 18. Comparison between extractable and total elemental concentrations vs. depth for Fe, Ni, Al, Cu, Mn, Mg, Cr, Zn and K.

can be calculated:

$$(\text{mass of metal}) = \int_0^L c(x)\mathrm{d}x \cdot \rho_b \mathrm{WH} \tag{4}$$

The results suggest that large amounts of potentially toxic metals may be released if the oxidized tailings are reductively dissolved (Table 9). The total masses of Ni and Cr available for reductive dissolution in the western portion of the tailings are 13 t Ni and 15 t Cr. The masses of Co, Zn and Pb are smaller. Furthermore, the Fe(II) released by reductive dissolution can react with oxygen when discharged from the anaerobic tailings to the oxic surface-water flow system. In this case, two moles of H^+ are produced for each mole of Fe(II), according to reactions (1) and (2). These reactions indicate that a net $2.5 \cdot 10^8$ mol of H^+ will be produced if all of the Fe(II) is oxidized. The extent of acidic conditions generated will depend on the rate of release of this water and the amount of dilution with surface water.

The actual masses of metals and H^+ ions that can be released into the pore water, and the rate of this release, depend on several site-specific characteristics, particularly the size of the impoundment and the intensity of the reducing conditions established near the tailings surface. The surface area of the Nickel Rim impoundment is relatively small, and other impoundments may contain masses of metals several

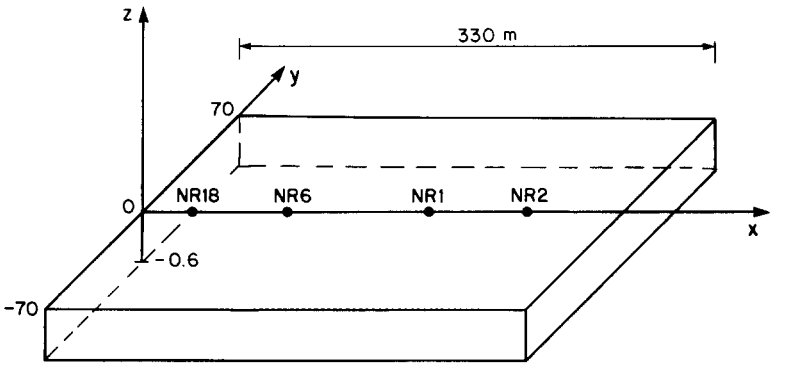

Fig. 19. Volume of tailings used to estimate the total masses of metals in the oxidized zone of the Nickel Rim impoundment.

orders of magnitude greater than those estimated in this study. Further experiments are required to assess the extent and the kinetics of reductive dissolution of Fe(III)-(oxy)hydroxides by organic acids, typical of those derived from organic-rich O_2-consuming cover materials and under conditions representative of the tailings environment.

7. Conclusions

Organic acids from covered tailings with organic-carbon-rich material may reductively dissolve Fe(III)-(oxy)hydroxides contained in the weathered tailings, thereby releasing potentially toxic metals previously adsorbed onto or coprecipitated with the Fe(III)-(oxy)hydroxides. A methodology was developed to extract the metals contained in two chemical fractions of the tailings, a water-soluble fraction and a reducible fraction. Samples from the Nickel Rim mine-tailings impoundment indicate that the water-soluble fraction contains a very small amount of metals compared to that of the reducible fraction.

The reducible fraction, which is composed mainly of Fe(III)-(oxy)hydroxides,

Table 9
Masses of metal contained in upper 60 cm of the western part of Nickel Rim mine tailings impoundment

Metal	Mass	Mass/area ($t\ ha^{-1}$)
Fe	7,050	1,570
Ni	13	2.8
Cu	20	4.5
Cr	15	3.4
Co	1	0.2
Mn	9	2
Pb	0.6	0.2
Zn	2	0.5

represents a large percentage of the total metal content of the tailings. In the oxidized zone of the tailings, >80% of Fe, Ni, Cu, Cr and Co potentially is available for release by reductive-dissolution reactions. The total mass of metals potentially available for release by reductive dissolution of the Fe(III)-(oxy)hydroxides contained in the 4.5-ha western half of the Nickel Rim mine tailings impoundment is estimated to be more than 7000 t of Fe, between 10 and 20 t each of Ni, Cu, Cr and Mn, and between 0.5 and 2 t of Co, Zn and Pb. Because Fe is released to the pore water as ferrous iron, which oxidizes when leaving the anaerobic conditions of the covered tailings, the acid production may be substantial. These results suggest that the use of an organic cover over oxidized tailings to stop any further sulphide oxidation may increase the magnitude of the environmental problems it is designed to prevent.

Acknowledgements

We thank Ling Zhang for her assistance in performing the AAS analyses. Core samples for this study were provided by R.H. Johnson and W.D. Robertson, University of Waterloo. This study was supported in part by Falconbridge Ltd. and by the Natural Science and Engineering Research Council of Canada.

References

Arnold, R.G., DiChristina, T.J. and Hoffmann, M.R., 1988. Reductive dissolution of Fe(III) oxides by *Pseudomonas* sp. *200*. Biotechnol. Bioeng., 32: 1081–1096.

Blenkinsopp, S.A., Herman, D.C. and Costerton, J.W., 1991. The use of biofilm bacteria to exclude oxygen from acidogenic mine tailings. 2nd Int. Conf. on Abatement of Acidic Drainage, Montréal, Qué., 1: 369–377.

Blowes, D.W., 1990. The geochemistry, hydrogeology and mineralogy of decommissioned sulfide tailings: A comparative study. Ph.D. Thesis, University of Waterloo, Waterloo, Ont.

Blowes, D.W. and Jambor, J.L., 1990. The pore-water geochemistry and the mineralogy of the vadose zone of sulfide tailings, Waite Amulet, Québec, Canada. Appl. Geochem., 5: 327–346.

Blowes, D.W., Reardon, E.J., Jambor, J.L. and Cherry, J.A., 1991. The formation and potential importance of cemented layers in inactive sulfide mine tailings. Geochim. Cosmochim. Acta, 55: 965–978.

Blowes, D.W., Jambor, J.L., Appleyard, E.C., Reardon, E.J. and Cherry, J.A., 1992. Temporal observations of the geochemistry and mineralogy of a sulfide-rich mine-tailings impoundment, Heath Steele Mines, New Brunswick. Explor. Min. Geol., 1: 252–264.

Brock, T.P., Smith, D.W. and Madigan, M.T., 1984. Biology of Microrganisms. Prentice-Hall, New York, NY, 847 pp.

Broman, P.G., Haglund, P. and Mattson, E., 1991. Use of sludge for sealing purposes in dry covers: Development and field experiences. 2nd Int. Conf. on Abatement of Acidic Drainage, Montréal, Qué., 1: 515–527.

Brown, A., 1991. Proposal for the mitigation of acid leaching from tailings using a cover of muskeg peat. 2nd Int. Conf. on Abatement of Acidic Drainage, Montréal, Qué., 2: 517–527.

Dos Santos Alfonso, M., Morando, P.J., Blesa, M.A., Banwart, S. and Stumm, W., 1990. The reductive dissolution of iron oxides by ascorbate: The role of carboxylate anions in accelerating reductive dissolution. J. Colloid Interface Sci., 138: 74–82.

Freeze, R.A. and Cherry, J.A., 1979. Ground Water. Prentice-Hall, Englewood Cliffs, NJ, 604 pp.

Garrels, R.M. and Christ, C.L., 1965. Solutions, Minerals, and Equilibria. Freeman & Cooper, San Francisco, CA, 449 pp.

Gibbs, M.M., 1979. A simple method for the rapid determination of iron in natural waters. Water Res., 13: 295–297.

Jambor, J.L. and Owens, D.R., 1993. The mineralogy of the tailings impoundment at the former Cu–Ni deposit of Nickel Rim Mines Ltd., eastern edge of the Sudbury Structure, Ontario. Energy, Mines & Resour., Can., CANMET (Can. Cent. Miner. Energy Technol.) Div. Rep. MSL 93-4 (CF).

Johnson, R., 1993. The hydrogeology and geochemistry of the Nickel Rim mine tailings impoundment, Sudbury, Ontario. M.Sc. Thesis, University of Waterloo, Waterloo, Ont.

Jones, J.G., Gardener, S. and Simon, B.M., 1983. Bacterial reduction of ferric iron in a stratified eutrophic lake. J. Gen. Microbiol., 129: 131–139.

Jones, J.G., Gardener, S. and Simon, B.M., 1984. Reduction of ferric iron by heterotrophic bacteria in lake sediments. J. Gen. Microbiol., 130: 45–51.

LaKind, J.S. and Stone, A.T., 1989. Reductive dissolution of goethite by phenolic reductants. Geochim. Cosmochim. Acta, 53: 961–971.

Lovley, D.R., 1987. Organic matter mineralization with the reduction of ferric iron: A review. Geomicrobiol. J., 5: 375–399.

Lovley, D.R. and Lonergan, D.J., 1990. Anaerobic oxidation of toluene, phenol, and *p*-cresol by the dissimilatory iron-reducing organism GS-*15*. Appl. Environ. Microbiol., 56: 1858–1864.

Lovley, D.R. and Phillips, E.J.P., 1988. Novel mode of microbial energy metabolism: Organic carbon oxidation coupled to dissimilatory reduction of iron or manganese. Appl. Environ. Microbiol., 54: 1472–1480.

Lovley, D.R. and Phillips, E.J.P., 1989. Requirements for a microbial consortium to completely oxidize glucose in Fe(III)-reducing sediments. Appl. Environ. Microbiol., 55: 3234–3236.

Lovley, D.R., Baedecker, M.J., Lonergan, D.J., Cozzarelli, I.M., Phillips, E.J.P. and Siegel, D.I., 1989a. Oxidation of aromatic contaminants coupled to microbial iron reduction. Nature (London), 339: 297–299.

Lovley, D.R., Phillips, E.J.P. and Lonergan, D.J., 1989b. Hydrogen and formate oxidation coupled to dissimilatory reduction of iron or manganese by *Alteromonas putrefaciens*. Appl. Environ. Microbiol., 55: 700–706.

Nirel, P.M.V. and Morel, F.M.M., 1990. Pitfalls of sequential extractions. Water Res., 24: 1055–1056.

Pitchel, J.R. and Dick, W.A., 1991. Influence of biological inhibitors on the oxidation of pyritic mine spoil. Soil Biol. Biochem., 23: 109–116.

Starr, R.C. and Ingleton, R.A., 1992. A new method for collecting samples without a drill rig. Ground Water Monit. Rev., Winter Iss., pp. 91–95.

Stone, A.T., 1987a. Microbial metabolites and the reductive dissolution of manganese oxides: Oxalate and pyruvate. Geochim. Cosmochim. Acta, 551: 919–925.

Stone, A.T., 1987b. Reductive dissolution of manganese (III, IV) oxides by substituted phenols. Environ. Sci. Technol., 21: 979–988.

Stone, A.T. and Morgan, J.J., 1984a. Reduction and dissolution of manganese(III) and manganese(IV) oxides by organics, 1. Reaction with hydroquinone. Environ. Sci. Technol., 18: 450–456.

Stone, A.T. and Morgan, J.J., 1984b. Reduction and dissolution of manganese(III) and manganese(IV) oxides by organics: 2. Survey of the reactivity of organics. Environ. Sci. Technol., 18: 617–624.

Stone, A.T. and Ulrich, H.J., 1989. Kinetics and reaction stoichiometry in the reductive dissolution of manganese(IV) dioxide and Co(III) oxides by hydroquinone. J. Colloid Interface Sci., 132: 509–522.

Suter, D., Siffert, C., Sulzberger, B. and Stumm, W., 1988. Catalytic dissolution of iron(III) (hydro)oxides by oxalic acid in the presence of Fe(II). Naturwissenschaften, 75: 571–573.

Tessier, A. and Campbell, P.G.C., 1988. Comments on the testing of the accuracy of an extraction procedure for determining the partitioning of trace metals in sediments. Anal. Chem., 1475–1476.

Tessier, A. and Campbell, P.G.C., 1991. Comment on "Pitfalls of sequential extractions", by P.M.V. Nirel and F.M.M. Morel. Water Res., 115–117.

Tessier, A., Campbell, P.G.C. and Bisson, M., 1979. Sequential extraction procedure for the speciation of particulate trace metals. Anal. Chem., 51: 844–851.

Tessier, A., Rapin, F. and Carignan, R., 1985. Trace metals in oxic lake sediments: possible adsorption onto iron oxyhydroxides. Geochim. Cosmochim. Acta, 49: 183–194.

Tessier, A., Carignan, R., Dubreuil, B. and Rapin, F., 1989. Partitioning of zinc between the water column and the oxic sediments in lakes. Geochim. Cosmochim. Acta, 53: 1511–1522.

Zinder, B., Furrer, G. and Stumm, W., 1986. The coordination chemistry of weathering, II. Dissolution of Fe(III) oxides. Geochim. Cosmochim. Acta, 50: 1861–1869.